

A Six-Phase Multilevel Inverter for MEMS Electrostatic Induction Micromotors

Timothy C. Neugebauer, *Student Member, IEEE*, David J. Perreault, *Member, IEEE*, Jeffrey H. Lang, *Fellow, IEEE*, and Carol Livermore, *Member, IEEE*

Abstract—The construction of miniaturized rotating electric machines through microfabrication techniques is becoming a reality. Applications of such micromotors include miniaturized pumps, compressors, fans, coolers, and turbogenerators. However, the characteristics of these devices make the design of power electronics for them challenging. These characteristics include high-voltage and high frequency operation, tightly constrained operating waveforms and timing, and capacitive input impedances. This paper explores the design of power electronics for microfabricated electrostatic induction machines. We describe the structure and operation of these machines, and establish the operating requirements of power converters for them. We provide a comparison of inverter topologies for this application, and propose an appropriate architecture. The design and experimental evaluation of a prototype six-phase, five-level inverter for this application is presented. The inverter operates at frequencies up to 2 MHz and at voltages up to 300 V, and meets the stringent waveform and timing constraints posed by this application.

Index Terms—Electric induction motors, electrostatic micromotors, microelectromechanical systems (MEMS), multilevel inverter, power electronics.

I. INTRODUCTION

MICROELECTROMECHANICAL systems (MEMS) technology promises to enable the development of a wide range of miniaturized sensors and actuators. MEMS systems are implemented through batch microfabrication, or micromachining, techniques that have evolved from those used to fabricate integrated circuits. Rotating electrical machines implemented through microfabrication techniques are becoming practical [1]–[3]. Applications of such micromotors include miniaturized pumps, compressors, fans, coolers, and turbogenerators.

Microelectromechanical sensors and actuators have a number of characteristics that make the design of power electronics for these devices challenging. These characteristics often include high-voltage and high frequency operation, tightly constrained operating waveforms and timing, and capacitive input characteristics. Furthermore, the desire to achieve system-level miniaturization can introduce an additional burden, as the power electronics often dominate the overall system size. The development of power electronic technologies and designs that address these challenges is crucial if MEMS technology is to realize its full potential.

Manuscript received March 10, 2002; revised November 20, 2002, July 12, 2003. This work was supported in part by the Defence Advanced Research Projects Agency (DARPA) under Contract DABT63-98-C-0004, and in part by the Army Research Office. The paper was recommended by Associate Editor S. Baglio.

The authors are with the Massachusetts Institute of Technology, Cambridge, MA 02139 USA (e-mail: neugebat@mit.edu).

Digital Object Identifier 10.1109/TCSII.2003.822419

This paper explores the design of power electronics for microfabricated electrostatic induction machines. The electrostatic, or electric, induction machine is the dual of the magnetic induction machine and, thus utilizes electric rather than magnetic forces [1]–[3]. The operating requirements of this machine present tremendous challenges to the design of the necessary power electronics. We expose these issues, and develop a design approach that begins to address them. The design and experimental evaluation of a six-phase, five-level inverter for this application is presented. The inverter operates at frequencies up to 2 MHz and at voltages up to 300 V, and meets the stringent waveform and timing constraints posed by this application.

The paper is organized as follows. Section II of the paper describes the structure and operation of electrostatic induction machines, and outlines the operating requirements of power converters for them. Section III proposes a multilevel inverter topology for this application, and describes the design of the converter power stage. The design of the converter control circuitry is described in Section IV. Section V presents experimental results that demonstrate the viability and high performance of the proposed design. Section VI evaluates the proposed approach, and considers future developments that are necessary in this area. Finally, Section VII concludes the paper.

II. ELECTROSTATIC INDUCTION MACHINE

Fig. 1 illustrates the structure and operation of a planar microfabricated electrostatic induction machine [2], [3]. On one side of its air gap are stator electrodes supported by an insulator deposited on a conducting substrate. The stator electrodes are interconnected to form six phases. On the other side of the air gap is the rotor, which rotates as a disk. The rotor consists of a conducting film supported by an insulator deposited on a conducting substrate. The power electronics excite the stator electrodes to produce a potential wave that travels around the stator. For motoring operation, the speed of the traveling wave exceeds that of the rotor. This wave, and the corresponding charges on the stator electrodes, induces image charges on the rotor surface across the airgap. The rotor charges lag behind the potential wave to produce a tangential electric field. This tangential field interacts with the rotor charges to induce a motoring torque. In generating operation, the rotor speed exceeds that of the traveling potential wave, and generating torque is produced. The simplest lumped-parameter model for such a machine is a capacitance in series with a resistance for each phase, where the resistance depends upon the slip speed of the machine. For the micromotors considered here, 30 pF per phase is a reasonable model for the capacitance.

It is important to maximize the power conversion capability of the electric machine, since it is the likely power bottleneck

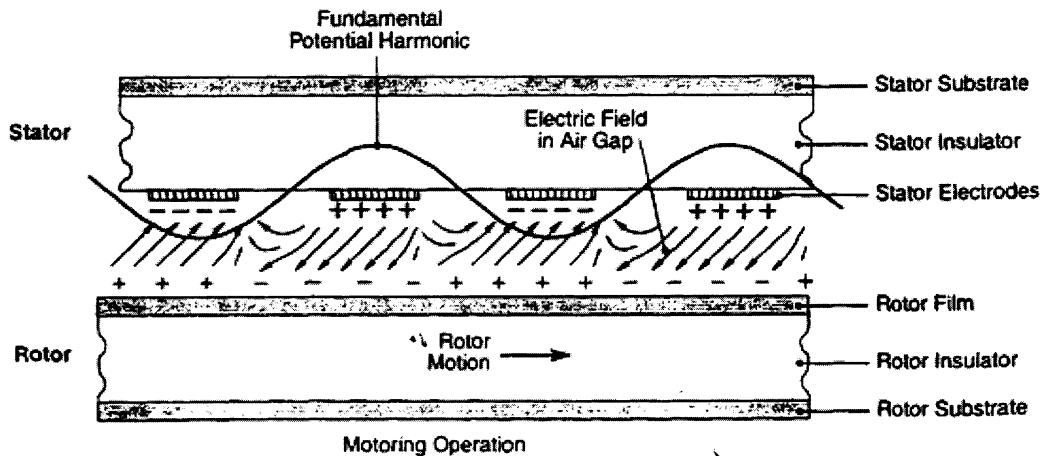


Fig. 1. Sideview of a microfabricated electrostatic induction machine. The electric charge and fields within the machine are also illustrated.

in most electrified microturbomachinery. To this end, it is desirable to run the machine at high torque and high speed, since both torque and speed contribute to power. High torque is achieved by operating the machine at the highest possible phase voltage. This voltage is limited by electrical breakdown [1] to approximately 300 V. High torque is also achieved with a machine that has a high spatial rate of energy conversion, that is, with a machine that has many poles. Here, lithography limits the number of poles to near 130. High speed is achieved through the use of air bearings. To date, we have run micro air bearings at over 1.1 Mrev/min, and hope to run them near 1.5 Mrev/min. This places a significant demand on the power electronics since the synchronous frequency of a 130-pole machine running at 1.5 Mrev/min is over 3 MHz.

Electrical breakdown considerations also dictate the number of phases that the machine must have. Not only must the line-to-neutral voltage of each phase be limited to 300 V, the *instantaneous* line-to-line voltage of neighboring phases must be limited to 300 V. To achieve this without limiting the line-to-neutral voltage, and hence limiting torque, requires a machine with six or more phases. Since an increased phase count requires finer-scale lithography, a six-phase design is utilized. Furthermore, operating constraints require that the phase voltages be accurate to within a few percent in magnitude and a few electrical degrees in phase. Phase accuracy is a particular challenge since an electrical degree is less than 1 ns at 3 MHz.

III. POWER CONVERTER DESIGN

Power converter design for such micromotors is clearly very challenging. A six-phase inverter capable of generating precise waveforms at multi-megahertz frequencies and hundreds of volts is needed. In this paper we address the design of an inverter that can generate balanced six-phase output voltages with magnitudes from 0–300 V over the frequency range 200 kHz–2 MHz. The generated phase voltages are sufficiently smooth that the prescribed line-to-line voltage limits are met at every point in time. Furthermore, the phase voltages are accurate to within 1.5 percent in magnitude, and to within 4° of phase across the operating range.

A. Power Stage Topology

Here we consider topologies for micromotor inverters. Tuned RF power amplifier structures (such as classes *D*, *E*, and their derivatives [4]–[6]) do not operate well over the wide frequency and load ranges considered here. Two-level pulse-width modulated bridge inverters are also not well suited to this application. A two-level inverter would need to employ a modulation frequency substantially higher than the fundamental ac frequency (along with an appropriate output filter) to achieve the smooth phase voltages that are required. Such high modulation frequencies are difficult to attain even with soft switching techniques, and realizing an appropriate modulation scheme would be equally difficult. Some form of multilevel inverter is more appropriate. General advantages of multilevel inverters include high purity output waveforms, low individual device switching frequencies, and reduced individual device blocking voltage requirements [7], [8]. All of these advantages are valuable in the present application. Nevertheless, many of the multilevel structures that are widely considered for high power applications—including diode-clamped converters, flying capacitor converters, and cascade converters [7]–[9]—are not well suited to the micromotor application. Limitations of these systems for this application include control complexity, difficulty of achieving sufficiently accurate switch timing due to level-shifting constraints, and the undesirable effects of parasitic capacitances between ground and the “flying” nodes of these circuits.

We propose a multilevel converter architecture having a high degree of modularity that avoids many of these limitations. The six phases are implemented with identical single-phase multilevel inverters. Each single-phase multilevel inverter is in turn constructed from a number of identical transformer-coupled full-bridge converters. The structure of the single-phase multilevel inverter is illustrated in Fig. 2. The full-bridge converters share a common dc-side voltage, and each full bridge drives the primary side of a transformer via a coupling capacitor. The secondary sides of the transformers are connected in series to form the output voltage for one phase. Each N -level single-phase inverter is comprised of $N - 1$ full-bridge converters and associated transformers. In the prototype system, four full bridges are used to form a five-level (9-step) single-phase inverter for

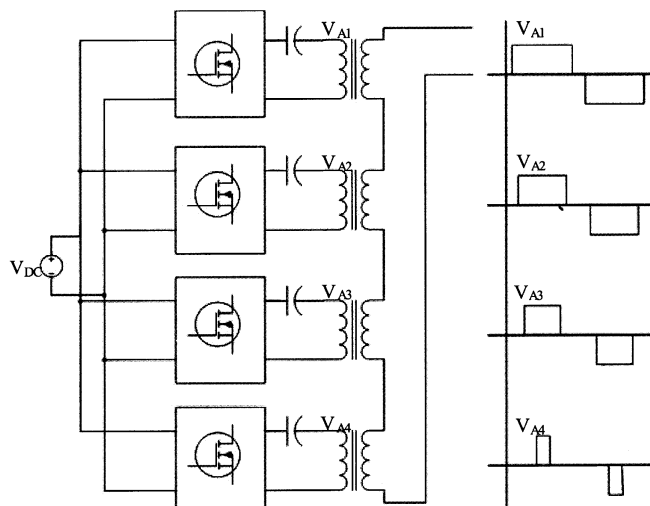


Fig. 2. Structure of the power stage for a single phase. Each phase consists of four full bridge inverters (see Fig. 3). Each inverter produces a different three-level voltage signal on the primary of the transformer. The secondaries of these transformers are in series, thereby summing these four signals into a nine-level sinusoidal signal.

each of the six phases.¹ The prototype system utilizes discrete components, though much of the design could be integrated.

The topology of Fig. 2 has a number of advantages for micromotor applications. First, unlike other topologies providing a high number of levels [7]–[9], half of the switch drives are ground referenced, and the remaining half are shifted only one step level from ground. This permits minimal, matched switching delays, thus enabling the necessary precision in switch timing to be achieved. Second, only the power-stage nodes attached to the blocking capacitors and transformers experience rapid voltage transitions with respect to ground, and these voltages only transition by a single step level. This makes it easier to limit the impact of parasitic capacitances on system operation. Third, unlike many multilevel topologies, there are no capacitor voltage balancing issues, and “flying” isolated dc supplies are not necessary. Furthermore, the topology admits a simple modulation strategy that meets the demands posed by this application. Finally, the high degree of modularity in the topology is advantageous: it reduces the level of design complexity (and may facilitate partial integration of the design in the future), and greatly simplifies the task of matching logic and switching delays down to nanosecond levels.

B. Power Stage Design

A simplified schematic of the power stage for a single bridge of one phase is shown in Fig. 3. The dc bus is controlled over the range 0–75 V. N-channel MOSFETs (model ZVN3310A, 100 V, 10 Ω) were selected as the main power devices. Device selection was based on a tradeoff between conduction losses (related to device resistance) and switching losses (related to device capacitance). For low-frequency operation device conduction losses (due largely to transformer magnetizing current) are

¹A closely related approach is to synthesize three phases with single-phase inverters, and use transformers to synthesize the other three phases. This reduces the amount of control circuitry, but limits the ability to fine-tune the timing of the inverter waveforms.

dominant. For high-frequency operation, switching losses (including loss for both device and output capacitances) are dominant. The semiconductor devices were chosen to balance these loss mechanisms across the converter operating range.

A high-speed level shifter is used for each high side device. The input capacitance of the high side devices is large enough that the level-shifter output resistance must be kept low to minimize switching delay. The resistive losses associated with this simple level shifting scheme are significant; a more sophisticated approach would certainly be merited in an integrated or partially integrated design.

In order to create accurate waveforms great attention must be placed on the timing in the power stage. The maximum operating frequency of the inverter is 2 MHz, which corresponds to a period of 500 ns. The precision in the phase delays needed means that the switching times must be accurate to less than 10 ns. Thus, the signal paths for all of the switching control signals must be short and very well matched. All the signal paths were matched using gate drivers and buffers that were chosen for their short and consistent delay times. To compensate for the effects of the level shifter and prevent shoot-through conditions, the low-side signal path has an added delay that depends on the direction of switching. This delay provides approximately 15 ns of blanking time between the on times of the high and low devices in a leg.

The current through a given switching device depends on the load, the synthesized voltage magnitude, frequency and switch duty ratio, and the transformer magnetizing inductance. In the worst-case condition for conduction loss, a square wave at the lowest ac frequency (200 kHz) and largest magnitude (75 V) is applied to the transformer primary. In this case, the fundamental of the magnetizing current (through L_{μ}) will be 75.8 mA per millihenry of magnetizing inductance. Based on a tradeoff between device size and transformer size, a magnetizing inductance of approximately 4 mH was deemed appropriate. Other considerations include the need to have good transformer behavior at RF frequencies. To achieve the desired performance, five WB1010-PC miniature RF transformers (Coilcraft, Cary, IL) are connected in series to form each transformer.

IV. CONTROLLER DESIGN

Realization of the inverter controls is also challenging. The controller must generate switching commands to the inverter power stage such that balanced six-phase waveforms are synthesized at a fundamental frequency of up to two megahertz. The switching commands must result in ac waveforms that are precisely matched, have low total harmonic distortion (THD), and are accurate to within a few degrees of phase. Furthermore, dissipation constraints limit the switching devices to one switching cycle per ac output cycle. In the design considered here, the output voltage magnitude is regulated directly via the dc bus voltage. A dc bus voltage of 0–75 V enables synthesis of ac output waveforms with peak voltages of 0–300 V; the inverter controls only need to ensure that the six-phase waveforms are balanced in magnitude.

The controller can be broken down into three different sections as shown in Fig. 4. The first section generates sine and cosine reference waveforms at the desired frequency. The second section converts these sine and cosine waves into balanced six-

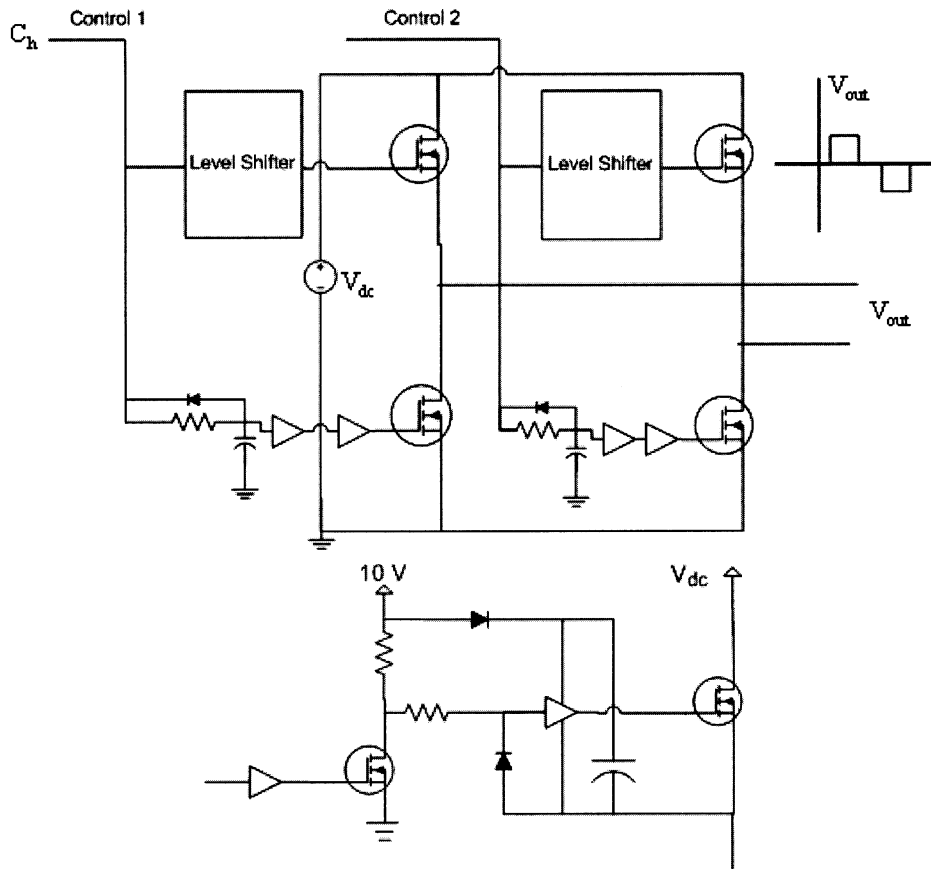


Fig. 3. (a) Simplified schematic of the full-bridge inverter used in the design. (b) Level shifter used to drive the high side switch. The 2 control signals (described in Fig. 4) regulate the four MOSFETs. The level shifter, which acts as an inverter, is needed to drive an n-type MOSFET which is not connected to ground. Extra delay elements are added to the gate of the other MOSFET so that the time delays between the signal and MOSFETs are uniform.

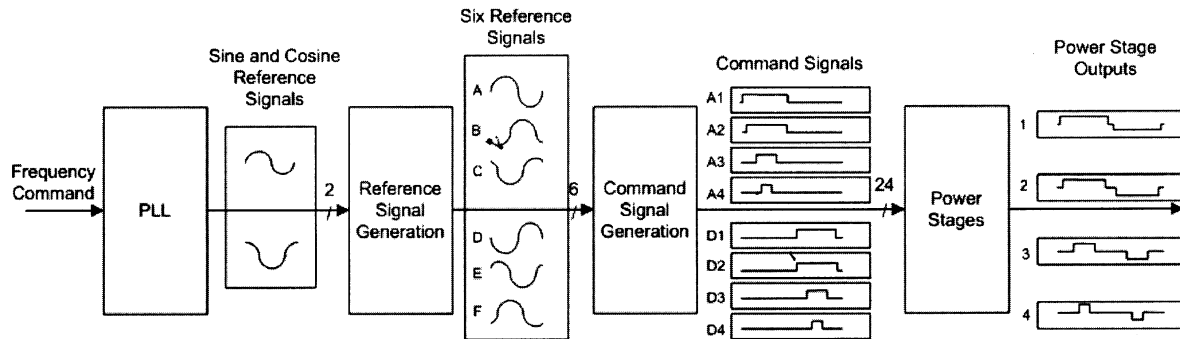


Fig. 4. Block diagram of the inverter controller and sample waveforms. The first stage takes a frequency command input and generates sine and cosine waveforms at that frequency. These two signals are linearly combined by the second controller stage to form balanced six-phase reference signals (six phases with 60° spacing). The third controller stage applies each of these reference signals to a set of high-speed comparators ordered to create twenty-four switching command signals. The command signals resulting from reference signals A and D are shown above. Opposite command signals (same duty cycle and 180° out of phase, for example A1 and D1) are sent to the power stage. These command signals create the appropriate three-step waveform for each bridge in the phase. The summation of the four output levels from an inverter phase results in a nine-step output.

phase sinusoidal references. The final section takes the sinusoidal reference for each phase and generates the appropriate switching waveforms for all devices of that phase.

In the first section of the controller, a phase-locked loop circuit generates two orthogonal sinusoidal signals at the commanded frequency (sine and cosine). This circuit needs to generate sinusoidal outputs with a precise 90° phase shift over a range from 200 kHz to 2 MHz. Taken together, these requirements are challenging. To meet them, two monolithic function generators are phase-locked in quadrature, as illustrated in

Fig. 5. To achieve both wide frequency control and tight phase control, two frequency adjust mechanisms are used in each function generator IC. The gross frequency adjust pins on both ICs are tied together so that adjustments in frequency affects them both. The second function generator is phase-locked in quadrature with the first one by placing its oscillator inside a phase-locked loop, and using its fine frequency adjustment input to control its phase relative to the first function generator.

The second section of the controller takes the sine and cosine reference signals and converts them to balanced six-phase sinu-

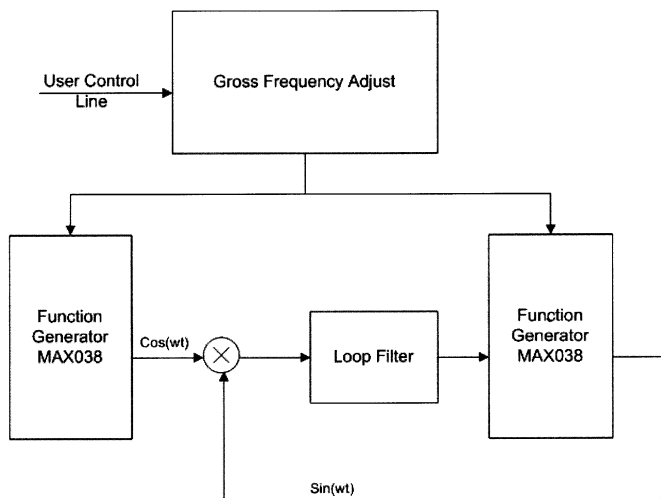


Fig. 5. Phase-locked loop has a one control line to set the frequency that interfaces with a frequency adjust pin within the function generators. A second frequency adjust pin is used as an input of the phase-locked loop. This circuit then is capable of stably creating two signals in quadrature over a wide frequency range.

soidal reference signals. All six reference signals are generated as linear combinations of the sine and cosine input. In the prototype system, means are provided for tuning the magnitude and phase balance of the six-phase waveforms. Each generated reference signal represents an ideal output waveform of one phase of the inverter.

The third section of the controller converts the reference voltage waveforms into modulation functions for each of the full-bridge converters. It must be recognized that switching signal timing must be accurate to within a few nanoseconds to achieve acceptable phase accuracy. This challenging task has been accomplished using high-speed comparator networks with adjustable switching thresholds. Figs. 2 and 4 illustrate the switching patterns for each of the bridges within a phase. The proposed patterns do not provide balanced dissipation among the bridges. However, they enable a single high-speed comparator to generate the switching signals for two bridge legs (in complementary phases), so that twenty-four comparators control modulation of the whole converter. In this scheme, one comparator compares a reference sinusoid to a tunable switching threshold. A second comparator compares the complementary reference sinusoid to an identical switching threshold. The outputs of these two comparators (e.g., A1 and D1 in Fig. 4) modulate a bridge in one phase and—reversed—modulate the corresponding bridge in the complementary phase. Four such switching functions are generated from each sinusoidal reference signal. This approach has proven to be fast, accurate, and easily to tune for high performance.

V. EXPERIMENTAL RESULTS

The prototype inverter is implemented with discrete components; a picture of the inverter and controls is shown in Fig. 6. It can synthesize ac waveforms into its rated load from 0–300 V over the frequency range 200 kHz to 2 MHz. The six-phase waveforms are accurate to within 1.5% in magnitude and 4°

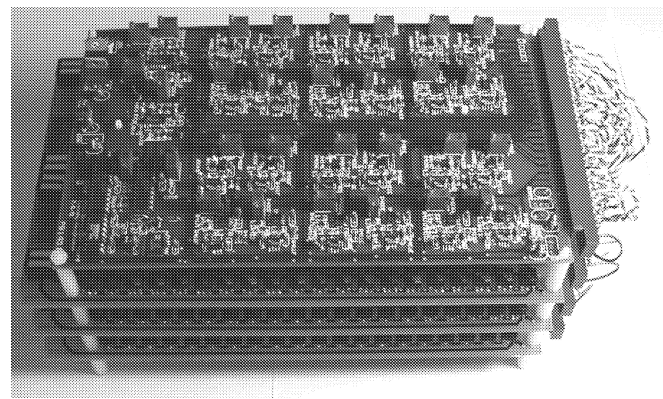
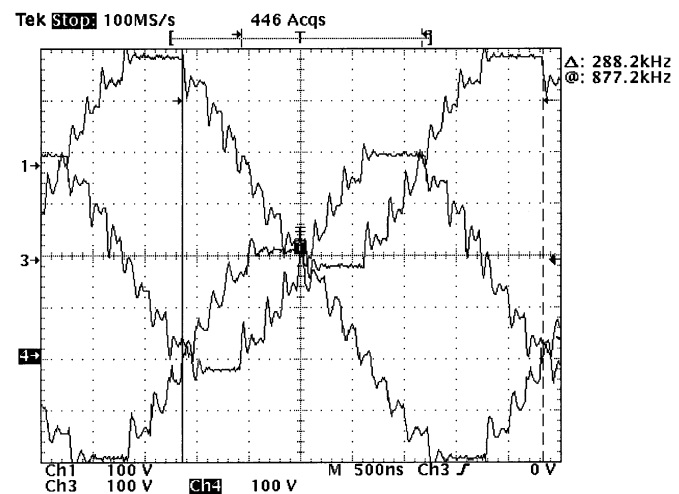
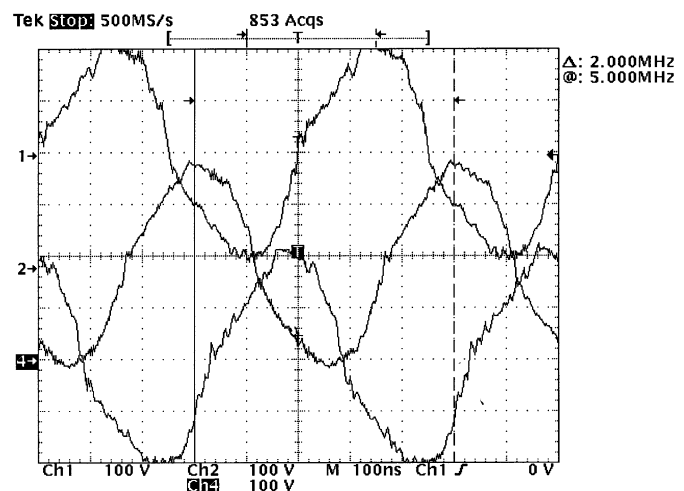


Fig. 6. Picture of the prototype inverter. The inverter is made up of four boards. The top board contains all the circuitry to create all the control signals. The three other boards each contain the power stages for two complementary output phases.



(a)



(b)

Fig. 7. Output voltages of three phases 120° out of phase and 400 V peak-to-peak. (a) At 288 kHz, the steps of the ideal waveform are visible. (b) At 2 MHz the waveform is more sinusoidal.

of phase over the operating range. The largest harmonic component is at least 19.8 dB (a factor of 9.8) below the fundamental. Fig. 7(a) shows three (120° out of phase) phases of the

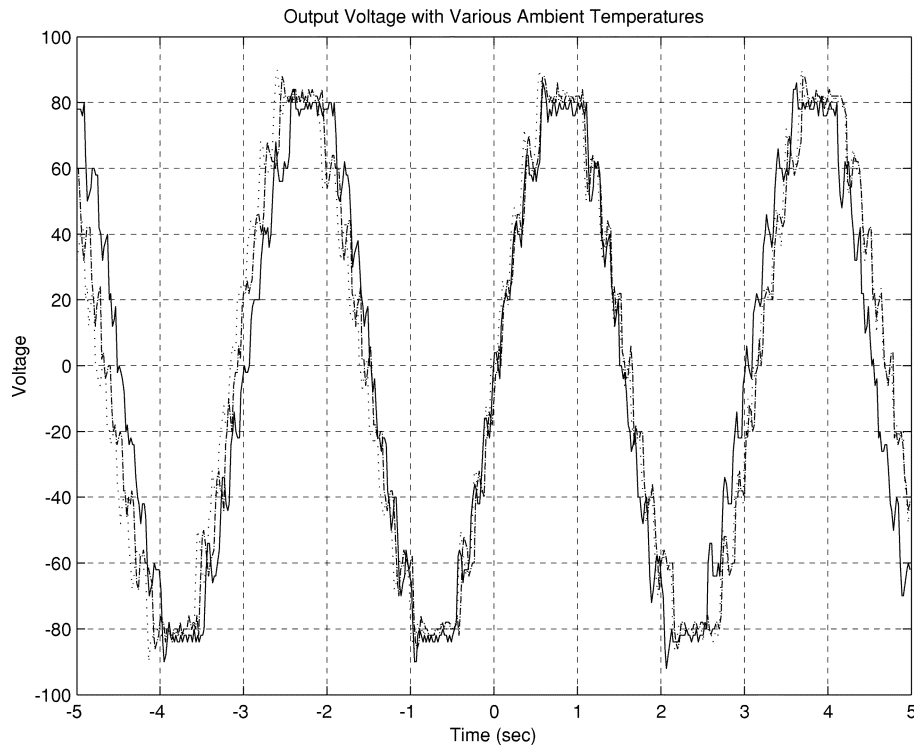


Fig. 8. Output voltage waveforms for operation at three ambient temperatures (6 °C, 22 °C, 40 °C). Slight frequency variation is the only major difference among waveforms across temperature.

converter output at 288 kHz. All nine steps of the synthesized waveform can be identified. Fig. 7(b) shows similar waveforms at 2 MHz. At high frequencies the transformer leakage inductances act with the capacitive load to filter the output waveform.

One issue that arose was nonuniform turn-on/turn-off times due to the level shifters. The high-side transistor's turn-on time is slightly longer than its turn-off time, and is different from that of the low-side device. This effect becomes pronounced at high voltage and high frequency, and results in an asymmetry in the output waveform under those conditions [visible in Fig. 7(b)]. This asymmetry itself does not greatly affect the overall system performance. To limit the instantaneous line-to-line voltages, however, the output voltage capability is derated from 300 V down to 250 between 1 and 2 MHz. An improved level-shifter design would eliminate this issue.

To ascertain the effects of temperature change on the inverter, a representative capacitive load was driven at three different ambient temperatures. As can be seen in the electrical waveforms of Fig. 8, the only significant effect of the ambient temperature change is a small change in frequency, due to the temperature sensitivity of the oscillator. The small variance is not expected to be of practical significance, and could easily be addressed with modification of the oscillator if needed.

Fig. 9(a) shows the output waveforms of the inverter driving a preliminary MEMs electrostatic machine. The prototype machine was operated using only two phases, and was driven both mechanically (with compressed air) and electrically (via the inverter) at speeds near 70 000 rpm (280 kHz electrical frequency). The inverter electrical waveforms are as expected. Fig. 9(b) shows preliminary data from the system. The change in machine speed induced by electrical excitation from the

inverter at 263 kHz is plotted against machine speed without electrical excitation. Operation in both the motoring and generating regimes is observed.

VI. EVALUATION AND FUTURE DIRECTIONS

The prototype system was designed to be able to drive micromechanical motors across a wide range of operating conditions while maintaining the waveform quality necessary in this application. In this regard, the proposed approach is entirely successful. However, the packaged converter is orders of magnitude larger than the associated MEMs motor. The prototype inverter consists of four separate pc boards: one board for each set of complementary phases and one board for control. Additional elements to the system are power supplies for the logic and gate drivers, fans for cooling, and an enclosure. An inverter for a practical MEMs motor drive application will have to be drastically reduced in size.

It is worthwhile to consider the extent to which miniaturization can be achieved in the context of the proposed approach. The total pc board area used in the prototype is 247 in², with 203 in² in logic and control, 18 in² in power switches, and 26 in² in magnetics. It is expected that the logic and control circuitry would be relatively easy to implement within a small integrated circuit. Reducing the area of the power devices represents a much greater challenge due to power dissipation constraints. One might reasonably expect to integrate a single bridge or perhaps a phase into an IC, but not an entire power stage. Nevertheless, substantial improvement in the size of the switching stage is expected to be possible with integration. It is the magnetics that represent the largest bottleneck for miniaturizing the

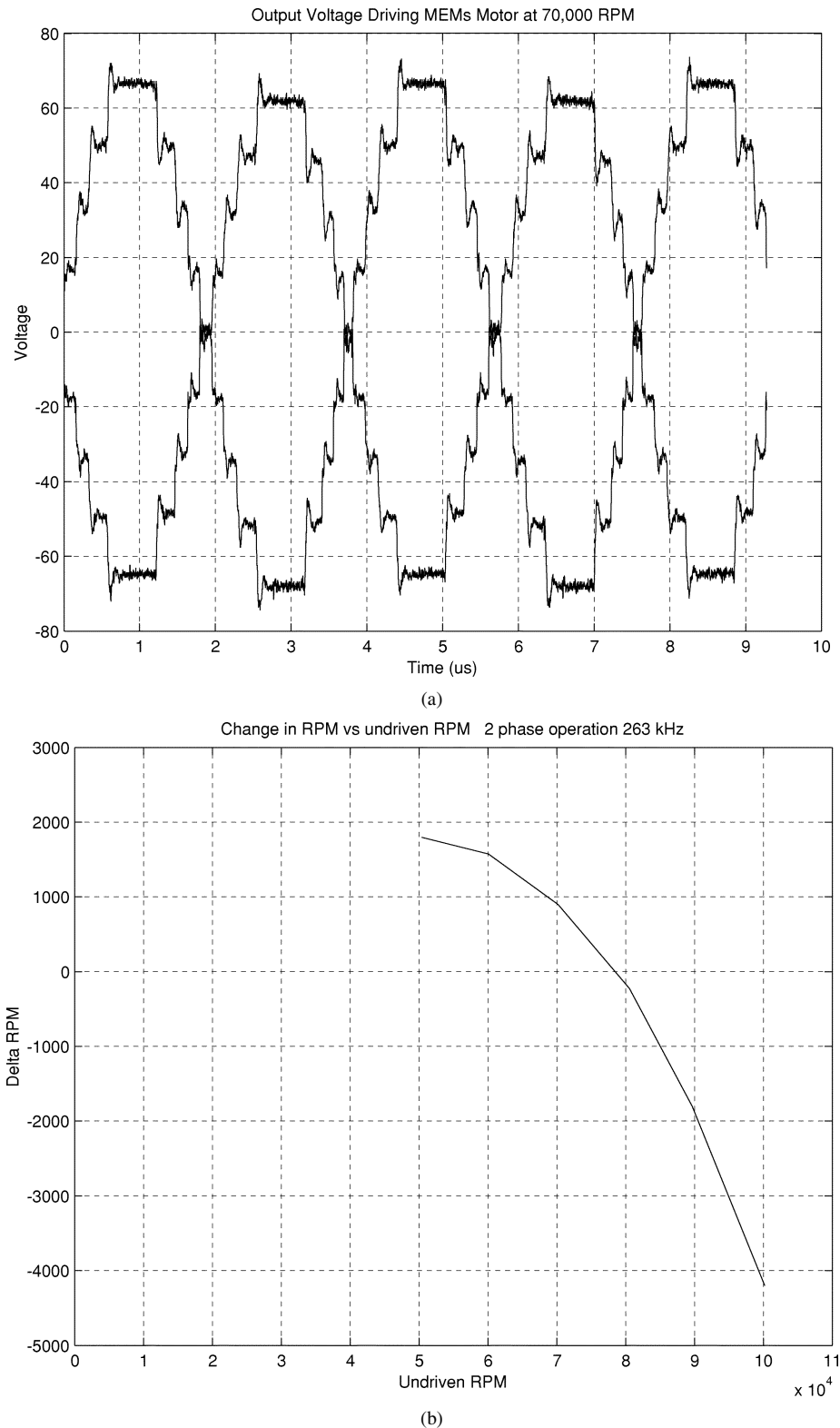


Fig. 9. (a) Output voltages of two phases at 150-V peak-to-peak while driving a MEMS machine near 70 000 rpm. (b) Preliminary data from the system showing change in machine speed versus machine speed.

proposed implementation. The proposed design utilizes approximately 6 in^3 of magnetics. Improved design of the magnetics might reduce this by a factor of two, but would result in the magnetics still being the dominant element in the system.

The prototype system was designed to operate over a wide frequency range. Restricting the design to a narrower frequency

range would result in large improvements in achievable size. First, if the operating range of the system were limited to the high-frequency regime (e.g., 1–2 MHz), the magnetizing inductance of the transformers could be reduced, with a commensurate reduction in transformer size. Second, limiting the frequency range would allow the switching devices to be

optimized for either low-frequency (conduction-dominated) or high-frequency (switching-dominated) operation (though improvements in the device sizing would not be independent of changes in the magnetics). One might expect to achieve a further factor of five to ten reduction in volume from such changes. This would still leave the converter as the dominant element in the MEMS, but might be acceptable in practical applications.

Other possibilities become apparent if the operating frequency range is further restricted. It is well known that the quality factor and power density of magnetics do not scale well to small sizes and are not very amenable to microfabrication techniques [10], [11]. If the MEMS machine drive is operated over a sufficiently narrow electrical frequency range, alternative energy storage and transformation mechanisms with different scaling properties—such as piezoelectric transformers [12]—might become practical. Furthermore, under narrowband conditions, some type of tuned inverter structure incorporating the machine capacitances might be useful. Such approaches remain to be fully explored.

VII. CONCLUSIONS

The construction of miniaturized rotating electric machines through microfabrication techniques is becoming a reality. Applications of such micromotors include miniaturized pumps, compressors, fans, coolers, and turbogenerators. However, the characteristics of these devices make the design of power electronics for them challenging. These characteristics include high-voltage and high frequency operation, tightly constrained operating waveforms and timing, and capacitive input impedances.

This paper explores the design of power electronics for microfabricated electrostatic induction machines. We describe the structure and operation of these machines, and establish the operating requirements of power converters for them. We provide a comparison of inverter topologies for this application, and propose an appropriate architecture. The design and experimental evaluation of a prototype six-phase, five-level inverter for this application is presented. The inverter operates across a wide range of frequencies up to 2 MHz and at voltages up to 300 V,

and meets the stringent waveform and timing constraints posed by this application. The limits of miniaturization of the proposed architecture are explored, and it is concluded that the magnetics in the design are the dominant limitation in miniaturization.

ACKNOWLEDGMENT

The authors would like to thank L. Steyn for his contributions to this work.

REFERENCES

- [1] S. F. Bart, T. A. Lober, R. T. Howe, J. H. Lang, and M. F. Schlecht, "Design considerations for micromachined electric actuators," *Sensors Actuators*, vol. 14, pp. 269–292, 1988.
- [2] S. F. Nagle and J. H. Lang, "A micro-scale electric-induction machine for a micro gas turbine generator," in *Proc. Conf. Electrostatics Society America*, Boston, MA, June 1999, pp. 57–66.
- [3] L. G. Fréchette, S. F. Nagle, R. Ghodssi, S. D. Umans, M. A. Schmidt, and J. H. Lang, "An electrostatic induction micromotor supported on gas-lubricated bearings," in *Proc. IEEE 14th Int. Micro Electro Mechanical Systems Conf.*, Interlaken, Switzerland, Jan. 2001.
- [4] P. J. Baxandall, "Transistor sine-wave LC oscillators," *Proc. IEE*, pt. B, vol. 106, pp. 748–758, 1959.
- [5] N. O. Sokal and A. D. Sokal, "Class E—A new class of high-efficiency tuned single-ended switching power amplifier," *IEEE J. Solid-State Circuits*, vol. 10, pp. 168–176, June 1975.
- [6] R. L. Steigerwald, "A comparison of half-bridge resonant converter topologies," *IEEE Trans. Power Electron.*, vol. 3, pp. 174–182, Apr. 1988.
- [7] J. S. Lai and F. Z. Peng, "Multilevel converters—A new breed of power converters," *IEEE Trans. Ind. Appl. Soc. (IAS)*, vol. 32, pp. 509–517, May/Jun. 1996.
- [8] F. Z. Peng, "A generalized multilevel inverter topology with self voltage balancing," *IEEE Trans. Ind. Applicat. Soc. (IAS)*, vol. 37, pp. 611–618, Mar/Apr. 2001.
- [9] F. Z. Peng, J. S. Lai, J. W. McKeever, and J. VanCoevering, "A multilevel voltage-source inverter with separate DC sources for static var generation," *IEEE Trans. Ind. Applicat. Soc. (IAS)*, vol. 32, pp. 1130–1138, Sept./Oct. 1996.
- [10] J. A. Ferriera and J. D. Van Wyk, "Electromagnetic energy propagation in power electronic converters: Toward future electromagnetic integration," *Proc. IEEE*, vol. 89, pp. 876–889, June 2001.
- [11] M. J. Prieto, A. M. Pernía, J. M. Lopera, J. A. Martín, and F. Nuño, "Design and analysis of thick-film integrated inductors for power converters," *IEEE Trans. Ind. Applicat. Soc. (IAS)*, vol. 38, pp. 543–552, Mar/Apr. 2002.
- [12] A. M. Flynn and S. R. Sanders, "Fundamental limits on energy transfer and circuit considerations for piezoelectric transformers," *IEEE Trans. Power Electron.*, vol. 17, pp. 8–14, Jan. 2002.